Characterization of the Panoramic Annular Lens

by D.L. Lehner, A.G. Richter, D.R. Matthys and J.A. Gilbert

ABSTRACT—The panoramic annular lens (PAL) consists of a single piece of glass, with spherical surfaces, that produces a flat annular image of the entire 360-deg surround of the optical axis of the lens. This paper describes the attributes of the PAL and shows that the lens maps elements from object to image space via a constant aspect ratio polar mapping. A panoramic video system (PVS) is described to illustrate how the characterization can be applied in experimental mechanics for cavity inspection and measurement.

Introduction

As shown in Fig. 1, the panoramic annular lens (PAL) is a single element imaging block comprising three spherical optical surfaces and one flat optical surface.[1] Two of the spherical surfaces are mirrored, while the third spherical surface and the flat surface are not. Rays leaving points A and B are refracted upon contacting the first spherical surface and reflect off the rear mirrored spherical surface. They travel forward in the lens and strike the front mirrored spherical surface. Reflected back, the rays are refracted at the rear flat optical surface and diverge as they exit the lens. The divergent rays leaving the flat optical surface at the back of the PAL can be "back traced" to form virtual images corresponding to points A and B at the points labeled A′ and B′. A biconvex lens, labeled as the collector lens, forms real images of these internal points at A″ and B″. Imaging all points contained within the field of view produces a flat annular image.

The PAL has been used extensively for making inspections and measurements within cylindrical cavities and pipes. The associated applications, collectively referred to as radial metrology, typically rely on visual inspection, structured light or coherent optical techniques.[2,3] In prior studies, however, attempts to quantitatively analyze and linearize PAL images have relied on the experimental determination of the mapping characteristics from object to image space; an analytical representation has not yet been established.

This paper describes the attributes of the PAL and presents an analytical formulation which shows that the PAL maps elements from object to image space via a constant aspect ratio polar mapping. The results of the analysis are compared to those obtained from experimental data and those obtained from the method of ray tracing. The paper concludes with a brief description of a system designed for cavity inspection that is based on this lens characterization.

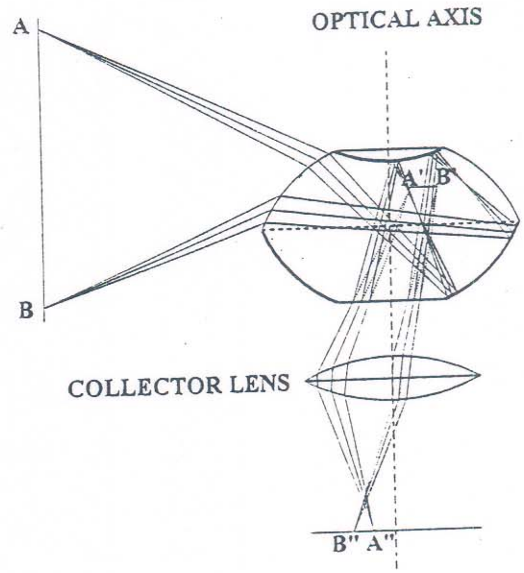

Fig. 1—Panoramic annular lens system

The Panoramic Annular Lens (PAL)

As illustrated in Fig. 2, the optical axis of the PAL is defined by a line perpendicular to the flat surface which passes through the centers of curvature of the three spherical surfaces. A longitudinal axis, labeled Z, is chosen to coincide with the optical axis. Two other axes, labeled X and Y, are established in a plane defined by the physical equator of the lens. They are chosen to form a right handed triad with the longitudinal axis. Spherical coordinates (ρ, α, θ) may also be defined with respect to the origin.

In Fig. 2, the angles α and θ are called the field angle and the radial position angle, respectively. The field angles corresponding to the points labeled A and B in Fig. 1 are called the upper and lower field angles, respectively. They define the limits on the field of view and are a function of the index of the glass used in the PAL.

Figure 3 shows a 38-mm (1.496-in.) diameter PAL made from Schott SF14 glass (n = 1.76), in which α_u = 65 deg and α_l = 110 deg. When the area between these field angles is rotated around the optical axis through a radial position angle of 2π, a cylinder is described. This continuous field of

D.L. Lehner is affiliated with the Optical Fabrication Branch, George C. Marshall Space Flight Center, Huntsville, AL 35812. A.G. Richter is a Graduate Student working in the Physics Department at Northwestern University, Evanston, IL 60208. D.R. Matthys (SEM Member) is a Professor in the Physics Department at Marquette University, Milwaukee, WI 53233. J.A. Gilbert (SEM Fellow) is a Professor in the Mechanical and Aerospace Engineering Department at the University of Alabama, Huntsville, AL 35899.

Portions of this work were presented at the 1995 SEM Spring Conference and Exhibit, Grand Rapids, MI, June 12-14, 1995.

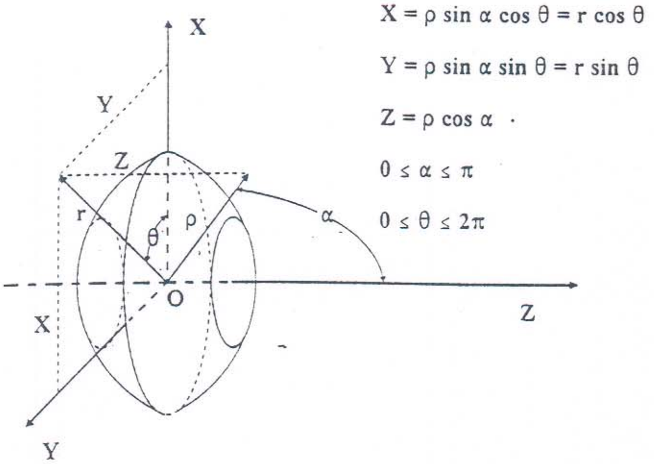

Fig. 2—Coordinate system and spherical coordinates used for radial metrology with a PAL

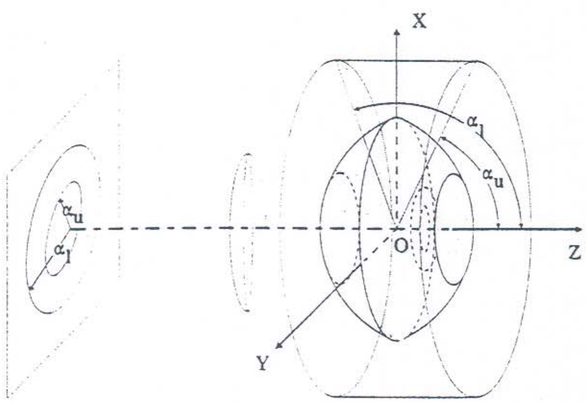

Fig. 3—Panoramic annular lens and its field of view

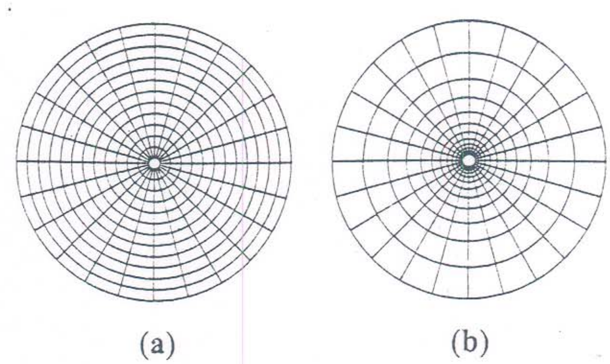

Fig. 4—A square grid wrapped around the inside wall of a cylinder becomes (a) a conventional polar map when recorded with a conventional lens and (b) a constant aspect ratio polar map when recorded with a PAL

view is mapped by a collector lens into a flat annular image. This PAL has been characterized in terms of spherical aberration and coma, distortion, image plane curvature and the modulation transfer function.[4] In general, the acceptance angle varies with the field angle; the amount of spherical aberration is proportional to the acceptance angle. The magnification varies quadradically, and image plane curvature is cubic.

From an experimental mechanics standpoint, the resolution of the PAL varies from the forward viewing edge to the back viewing edge with an angular resolution of approximately 6 millirads. Even though the PAL is not strictly afocal, objects appear to be in focus from the lens surface to infinity. The transmittance varies less than 5 percent over the visible light range; however, since the PAL is both refractive and reflective, it does not possess the same performance for all wavelengths.

Conventional Polar Mapping

In radial metrology, the aspect ratio of an area is defined as height divided by width. In real (or object) space, height is measured as the longitudinal distance relative to the optical axis of a lens; width corresponds to the circumferential distance measured around the optical axis. In image space, height is measured as a radial distance relative to the center of an image; width corresponds to a circumferential distance measured around the image center.

When a conventional lens is used for radial metrology, a cylinder, whose inside surface is composed of a uniform grid of squares, is mapped into the image plane as a series of evenly spaced concentric rings representing equally spaced lines drawn around the circumference of the cylinder; radial lines represent the longitudinal lines drawn along the length of the cylinder at constant circumferential positions.[5] Figure 4(a) illustrates that, in the case of the conventional lens, square elements having a real space aspect ratio of unity are mapped to an image comprising segments which have different image plane aspect ratios. The following section demonstrates that a PAL maps the same uniform grid of squares into the constant aspect ratio polar map illustrated in Fig. 4(b).

Constant Aspect Ratio Polar Mapping

Figure 5(a) shows a polar segment extracted from a polar mapping. The area of this segment can be written as

$$\text{AREA} = (\pi r_o^2 - \pi r_i^2)\phi \tag{1}$$

where ϕ is the fraction of a circle subtended, and is dimensionless. Factoring eq (1):

$$(\pi r_o^2 - \pi r_i^2)\phi = \pi\phi(r_o^2 - r_i^2) = \pi\phi(r_o - r_i)(r_o + r_i) \tag{2}$$

It can be seen in the figure that $(r_o - r_i)$ is equal to the radial height, Δr, of the section. The arc lengths s_o and s_i can be written as the product of their respective radial distances r_o and r_i, and θ—the angle they subtend measured in radians. Therefore, the term $(r_o + r_i)$ can be written as the sum of the arc lengths of the inside and outside edges of the element divided by θ. The angle ϕ is equivalent to θ divided by 2π. Finally, the sum of the arc lengths of the inside and outside edges of the element divided by two is equal to the arc length, (s_m), at the midpoint of the radial height of the element. These observations allow eq (2) to be rewritten as

$$\pi\phi(r_o^2 - r_i^2) = \pi\phi(\Delta r)\left(\frac{s_o + s_i}{\theta}\right) = \left(\frac{\theta}{2}\right)(\Delta r)\left(\frac{s_o + s_i}{\theta}\right)$$

$$= (\Delta r)\left(\frac{s_o + s_i}{2}\right) = (\Delta r)s_m \tag{3}$$

The above equation shows that the area of a polar segment is equal to the radial height times the midpoint arc length. Thus the area and aspect ratio for a polar type segment are given by

$$A \equiv \text{AREA} = \Delta r \; s_m$$

$$\kappa \equiv \text{ASPECT RATIO (POLAR SEGMENT)} = \frac{\Delta r}{s_m} \tag{4}$$

A polar map consisting of elements having constant polar aspect ratios can be constructed by considering Fig. 5(b), which shows two consecutive segments in the image plane. For these segments to subtend the same angle, the outside arc length of the inner element must be equal to the inside arc length of the outer element. Assuming the aspect ratios of the two elements to be equal,

$$\frac{\Delta r_1}{s_{1m}} = \frac{\Delta r_2}{s_{2m}} = \kappa \tag{5}$$

By rewriting eq (5) in terms of the inner and outer radius arc lengths, expressing these arc lengths as functions of radii drawn from the image center and rearranging terms we get

$$\frac{r_{1i}}{r_{1o}} + \frac{r_{2i}}{r_{2o}} + \frac{r_{1o}}{r_{2o}} \tag{6}$$

The above result can be used to determine the radial dimensions of subsequent polar segments once an initial segment has been established. The circumferential arc length of a polar element increases with increasing radial distance from the center of the map; consequently, the respective areas of sequential polar elements are different even when the aspect ratio of the elements remains constant.

An initial segment can be determined by picking a radial distance on the map and calculating the arc length subtended for a specific angle θ. Using this distance as the midpoint arc length for the segment, the following relationship can be written:

$$s_m = r_m\theta = \frac{\theta(r_i + r_o)}{2} \tag{7}$$

To retain constant perspective, the midpoint arc length must also be equal to the radial height of the element divided by the aspect ratio, which in equation form is

$$s_m = r_m\theta = \frac{\Delta r}{\kappa} = \frac{r_o - r_i}{\kappa} \tag{8}$$

Equating the right-hand sides of eqs (7) and (8)

$$\theta\left(\frac{r_i + r_o}{2}\right) = \frac{r_o - r_i}{\kappa} \tag{9}$$

and solving for r_o,

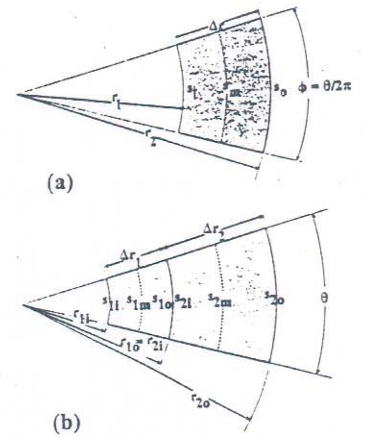

Fig. 5—(a) A typical segment generated from a polar map, (b) consecutive constant aspect ratio polar segments

$$r_o = r_i\left(\frac{2 + \kappa\theta}{2 - \kappa\theta}\right) \tag{10}$$

By substituting the latter into eq (9), it follows that

$$\frac{r_i}{r_o} = \frac{r_o}{r_?} \tag{11}$$

where $r_?$ is the outside radius of the next constant aspect ratio polar segment away from the center of the map. An alternative expression is

$$\frac{r_i}{r_o} = \frac{r_?}{r_i} \tag{12}$$

in which case $r_?$ is the inside radius of the next constant aspect ratio polar segment toward the center of the map.

The above procedure was followed to generate Fig. 4(b), which corresponds to a constant aspect ratio (with $\kappa = 1$) polar map for a cylinder with 24 divisions around the circumference (15-deg increments) and 12 units of longitudinal length.

Relationship between Object and Image Space

When a constant aspect ratio polar map is obtained in radial metrology, it is essential that the positions of points located in real space can be related to those in the image plane. To this end, consider the cylinder and the coordinate system shown in Fig. 6.

The axis collinear with the axis of the cylinder is labeled Z, and the orthogonal radial axes are labeled X and Y, respectively. The assumption is made that the upper edge of the cylinder is mapped to the inside radius of the polar map. The size of the radius chosen in the image plane defines the scaling factor for a geometrical construction and, in an actual PAL system, is determined by the magnification of the collector lens. The distance, d, measured from the upper edge of the cylinder to a given point located on the wall, is equivalent to a circumferential arc length, which may be computed using

$$d = r_{cyl}\theta \tag{13}$$

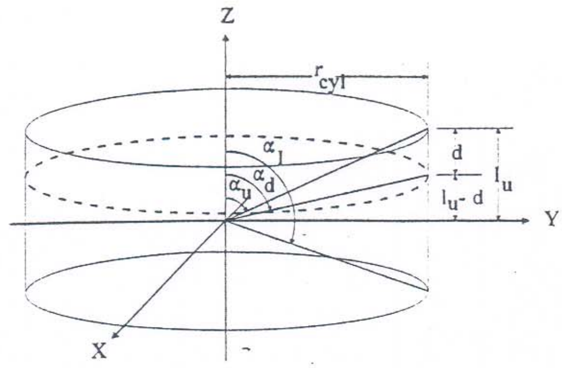

Fig. 6—Coordinate system axes and angles

where r_{cyl} is the radius of the cylinder. The corresponding radius on the polar map is obtained by solving eq (13) for θ and substituting into eq (10), which gives

$$r_d = r_i\left(\frac{2r_{cyl} + \kappa d}{2r_{cyl} - \kappa d}\right) \tag{14}$$

In practice, knowledge of the angular position with respect to the coordinate system provides important information even when the absolute dimensions of the cylinder are not known a priori. This knowledge can be obtained by considering Fig. 6 in which lines drawn from the origin to the upper and lower edges of the cylinder make angles of α_u and α_l, respectively, with the positive Z-axis. The angle formed by a line drawn from the origin to a point located at a distance, d, below the upper edge of the cylinder is α_d.

The angle α_u can be written in terms of the distance from the origin to the top of the cylinder as follows:

$$\cot(\alpha_u) = \frac{l_u}{r_{cyl}} \tag{15}$$

Angle α_d can be expressed in a similar fashion as

$$\cot(\alpha_d) = \frac{l_u - d}{r_{cyl}} = \frac{l_u}{r_{cyl}} - \frac{d}{r_{cyl}} \tag{16}$$

Substituting eq (15) into eq (16) and solving for d/r_{cyl}:

$$\frac{d}{r_{cyl}} = \cot(\alpha_u) - \cot(\alpha_d) \tag{17}$$

Solving eq (14) for d/r_{cyl}:

$$\frac{d}{r_{cyl}} = \frac{2}{\kappa}\left(\frac{r_d - r_i}{r_d + r_i}\right) \tag{18}$$

Setting the right-hand sides of eqs (17) and (18) equal and solving for $\cot(\alpha_d)$:

$$\cot(\alpha_d) = \cot(\alpha_u) - \frac{2}{\kappa}\left(\frac{r_d - r_i}{r_d + r_i}\right) \tag{19}$$

Finally, solving eq (19) for α_d:

$$\alpha_d = \tan^{-1}\left(\frac{\kappa(r_d + r_i)\tan(\alpha_u)}{\kappa(r_d + r_i) - 2(r_d - r_i)\tan(\alpha_u)}\right) \tag{20}$$

Equation (20) shows that when the angle from the origin to the upper edge of a cylinder is known in real space, the angle from the origin to any point can be determined from measurements taken in the image plane.

Verification of the Mapping Characteristic

An experimental procedure to determine the parameters necessary to compare the results predicted by the above equations with a photograph actually taken through the PAL was recently reported.[6] The PAL was mounted in a vertical position on a CCD video imaging system with a resolution of 512 × 512 pixels. Three vertical target boards were placed a constant distance from the optical axis of the lens at 120-deg spacings; this configuration ensured that the PAL was aligned with the targets. Marks were placed on the targets corresponding to the lowest and highest points that could be seen in the PAL image. The angles that the marks on the target made with respect to the optical axis of the lens were then calculated. Upper and lower field angles of 64 deg and 107.7 deg were obtained.

During these tests, the radii of the inside and outside edges of the annular image were found to be 100 and 188 pixels, respectively. Equation (19) can be rewritten to solve for the aspect ratio of the image (with r_o and α_o substituted for r_d and α_d) as follows:

$$\kappa = \left(\frac{2}{\cot(\alpha_u) - \cot(\alpha_o)}\right)\left(\frac{r_o - r_i}{r_o + r_i}\right) \tag{21}$$

An aspect ratio of 0.7574 is obtained when the values reported are substituted into this equation.

The first step in generating the polar map is to arbitrarily choose a value for the outer radius of the annular image. Then, eq (18) is rearranged to solve for the inside radius of the map as follows:

$$r_i = r_o\left(\frac{2 - \kappa(\cot(\alpha_u) - \cot(\alpha_o))}{2 + \kappa(\cot(\alpha_u) - \cot(\alpha_o))}\right) \tag{22}$$

Assuming that r_o = 6.99 cm (2.75 in.) and using κ = 0.7574, α_u = 64 deg, α_o = 107.7 deg, eq (22) gives a value r_i = 3.72 cm (1.463 in.). Equation (22) can be rearranged once more to establish the radial distances corresponding to the 15-deg grid squares as follows:

$$r_d = r_i\left(\frac{2 + \kappa(\cot(\alpha_u) - \cot(\alpha_o))}{2 - \kappa(\cot(\alpha_u) - \cot(\alpha_o))}\right) \tag{23}$$

The map shown in the lower half of Fig. 7 was obtained using eq (23) and reducing the field angle from 107.7 deg in 15-deg increments. The upper half of the figure shows a photograph taken through the PAL of a 15-deg grid of white and black squares placed in an actual cylinder. Slight differences between the upper and lower halves of the figure may be attributed to misalignment of the PAL in the cylinder and to the distortion caused by the collector lens.

An alternate method of verifying that the PAL produces a constant aspect ratio polar map is to compare the results obtained above with those obtained by ray tracing. In Ref. 4, the PAL was modeled with a ray-tracing program written specifically to accommodate the lens' unique geometry. Rays were traced from an imaginary cylinder through an analytical lens model, and the locations of the focus of groups of rays were plotted. The distance to vari-

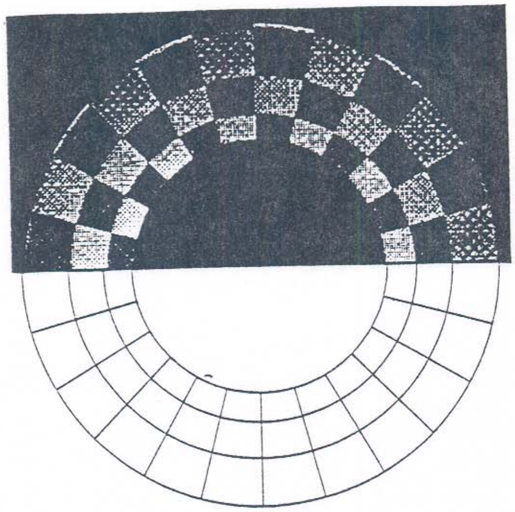

Fig. 7—A comparison of the analytical map to a photograph of a square grid taken through a PAL

ous points of focus from the inside radius of the annular image was determined by the location from which rays originated on the imaginary cylinder. By plotting numerous rays from different positions on the imaginary cylinder and their respective focal point locations, a graph showing the theoretical mapping function of the lens was generated. A third order curve was fit to the data; the mapping (or "linearization") function obtained was

$$\text{Image Height} = 0.1011\left(\frac{d}{r_{\text{cyl}}}\right) + 0.0691\left(\frac{d}{r_{\text{cyl}}}\right)^2 + 0.0084\left(\frac{d}{r_{\text{cyl}}}\right)^3 \quad (24)$$

In this case, the value of the distance measured from the highest visible edge of the cylinder to the point in question divided by the radius of the cylinder, d/r_{cyl}, ranged from 0.0 to 0.95; the image height was measured from the inside radius of the image outward.

A comparison can be made with the constant aspect ratio polar-mapping equations developed earlier using eq (15) twice: first to establish the aspect ratio for the map, and then to describe a continuous mapping function. The inside radius of the image, r_i, was reported to be equal to 3.49 mm (0.13738 in.).[5] The outside image radius, r_o, is found by adding the inside radius to the image height predicted by eq (24) at $\{d/r_{\text{cyl}}\}_{\max}$, as 7.70 mm (0.30299 in.). Solving eq (18) for κ, substituting the outside radius of the image for r_d, and using $\{d/r_{\text{cyl}}\}_{\max}$ gives the following expression for the aspect ratio:

$$\kappa = 2\left(\frac{r_o - r_i}{r_o + r_i}\right)\left(\frac{r_{\text{cyl}}}{d}\right)_{\max} \quad (25)$$

Substituting known values, $\kappa = 0.79173$.

Solving eq (18) for r_d gives an expression for the radial position of any point in the constant aspect ratio polar map from its cylindrical spatial position, as follows:

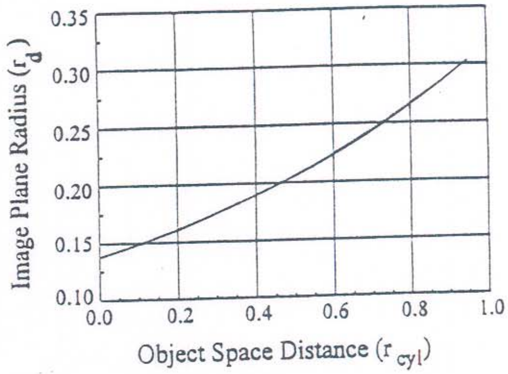

Fig. 8—A comparison between the analytical formulation and the method of ray tracing

$$r_d = r_i\left(\frac{2 + \kappa\left(\frac{d}{r_{\text{cyl}}}\right)}{2 - \kappa\left(\frac{d}{r_{\text{cyl}}}\right)}\right) \quad (26)$$

When a constant r_i term is added to eq (24), both it and eq (26) establish a mapping function from the center of the image outward. Equations (24) (with a constant r_i of 3.49 mm [0.13738 in.] added) and (26) were both evaluated for d/r_{cyl} ranging from 0.0 to 0.95, and are plotted for comparison in Fig. 8; the dashed line represents the modeled PAL, and the solid line represents constant aspect ratio polar mapping. The two curves agree to within 2 percent.

The Panoramic Video System (PVS)

The characterization of the PAL will be important in many areas of experimental mechanics. Figure 9, for example, shows a 7.62-cm (3.0-in.) diameter panoramic video system (PVS)[7] prepared as a deliverable under a NASA contract. The PVS relies on a PAL (1) to capture a cylindrical view of the region surrounding the lens through a transparent window (2). Incandescent illumination is distributed over the cylindrical field of view using a light ring (3) and an optical waveguide (4). Measurement capabilities are provided by projecting structured light into the field of view using a laser diode (5) and a rotating mirror driven by a motor (6). Panoramic images are acquired with a digitizing camera (7) and stored in a modified image enhancer. The enhancer includes menu driven image-processing soft-

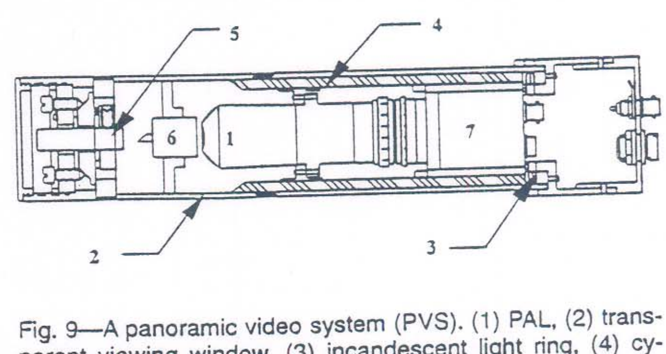

Fig. 9—A panoramic video system (PVS). (1) PAL, (2) transparent viewing window, (3) incandescent light ring, (4) cylindrical waveguide, (5) laser diode, (6) rotating mirror and motor, (7) digitizing camera

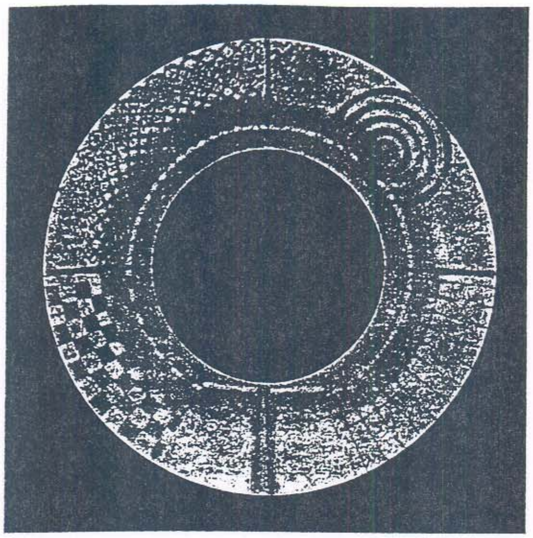

Fig. 10—The annular image of a test pattern and the laser trace over a flat cardboard inclusion obtained by placing the PVS along the longitudinal axis of a pipe

ware to linearize the annular images and make measurements within cavities.

Figure 10 shows the image of a test pattern obtained by placing the PVS along the longitudinal axis of a pipe having the pattern glued to its inner wall. A flat cardboard inclusion, placed in the lower section of the pipe, distorts the circular laser trace; the dark radial line in the center of the inclusion is the image of the wires, which supply power to the laser diode and the motor. The position of the laser trace is related to the radial distance between the optical axis of the PVS and the cavity wall; this relationship is based on the polar-mapping function developed herein.

Ongoing work with the PVS includes identifying and locating internal flaws, measuring the depth of surface cracks, comparing design contours to actual part contours, performing automated dimensional inspections and characterizing the geometrical relationships between components in complex assemblies. The PVS and some of these applications will be fully documented in the near future.

Conclusion

In conclusion, an analytical model was developed which predicts that the panoramic annular lens produces a constant aspect ratio polar mapping. The model was verified by comparing results with an actual photograph taken through the PAL and with the results obtained using a ray-tracing method. This characterization is important; it not only facilitates optical inspection and measurement through a PAL, but allows the PAL to be compared with other lenses. These comparisons will be made in the near future.

Acknowledgments

The authors would like to acknowledge the support provided by NASA's Marshall Space Flight Center, Marquette University and the University of Alabama in Huntsville. Lenses were provided to the project by Optechnology, Inc., Gurley, AL.

References

1. *Greguss, P., U.S. Patent No. 4,566,763 (1984).*
2. *Gilbert, J.A., Greguss, P., Lehner, D.L. and Lindner, J.L., "Radial Profilometry," Proc. Joint BSSM/SEM Int. Conf. on Adv. Strain Measurement Techniques, August 24-27, Whittles Publishing, London, 97-107 (1987).*
3. *Matthys, D.R., Gilbert, J.A. and Puliparambil, J., "Panoramic Holointerferometry,"* EXPERIMENTAL MECHANICS, **35** *(1), 83-88 (1995).*
4. *Richter, A.G., "Characterization of a Panoramic Annular Lens," MS thesis, Marquette University, Milwaukee, WI (1992).*
5. *Lehner, D.L., "Radial Metrology," PhD thesis, University of Alabama, Huntsville (1994).*
6. *Steadham, M.A., "Measurement of Spacecraft Attitude via the Panoramic Annular Lens Attitude Determination System (PALADS)," MS thesis, University of Alabama, Huntsville, (1994).*
7. *Lindner, C.H., "Cavity Inspection Using a Panoramic Annular Lens (PAL)," MS thesis, University of Alabama, Huntsville, (1994).*